

# A Modified Multiple Sample Correlation Algorithm for Electronic Target Location

Hélcio Vieira Junior

Electronic Warfare Center – CGEGAR, Brazilian Air Force – SHIS QI 05 Área Especial 12, 71615-600, Brasília, DF, Brazil.  
E-mail: junior\_hv@yahoo.com.br

**Abstract**—This research proposes a modification to the Multiple Sample Correlation Algorithm (MSCA) where some statistical concepts are aggregated to the original method. With our modifications we were able to improve the emitter position fix estimate more than 240% compared to the original MSCA and more than 1,200% compared to the Extended Kalman Filter Methodology.

**Index Terms**—Bearings-only target localization, Multiple Sample Correlation Algorithm, Triangulation.

## I. INTRODUCTION

The location's estimation of a stationary electronic emitter through using no more than passive bearing measurements has several purposes on the field of electronic warfare: surveillance, intelligence actions, interference location, and suppression of enemy air defense systems, among others.

This problem has been studied for decades and we can cite as recent works: [1-3].

There are two ways of estimating the emitter's localization: using the azimuth angle or using the time of arrival of an electronic signal. We will focus on the first method, which is called triangulation.

The triangulation method has several techniques: Geometrical, LSE (Least-Squared Error), DPD (Discrete Probability Density), Generalized Bearings, Maximum-Likelihood Estimation, and Multiple Sample Correlation. Readers are referred to [4] for an excellent survey on this subject.

In this work we suggest a modified approach to the Multiple Sample Correlation technique.

All the above applications on the field of electronic warfare are natural candidates for application of the proposed methodology and the users of our research are the electronic warfare's community.

This paper is organized as follows. In section 2, we review the Multiple Sample Correlation Algorithm. Our proposal is formally introduced in section 3. Section 4 presents preliminary computational results of the proposed technique

and section 5 concludes.

## II. MULTIPLE SAMPLE CORRELATION ALGORITHM

As mentioned before, the MSCA (Multiple Sample Correlation Algorithm) is one of the triangulation method's techniques. This methodology utilizes the azimuth angle of arrival of a signal, which is called line of bearing (LOB).

The aircraft (it can also be a ship or a ground vehicle) usually requires an antenna array to compute a LOB. It can use the signal phase, the signal relative amplitude or the signal time of arrival in order to perform this computation. Engineering limitations of the parameter measurement device (distance among the antennas, time measurement precision, and receiver sensibility, among others) create the measurement error and the atmosphere's perturbation on the signal creates the noise. The total error (measurement error plus the noise) makes the LOB to move away from the real emitter's bearing. For further details see [5].

The MSCA was proposed by Fu et al [6] and it "utilizes the intersection of the LOB fans, defined as the measured LOB plus and minus the maximum error in the sensor. Using the maximum error guarantees that the emitter is within the resulting area" [4]. This concept is illustrated in figure 1, where the circle represents the aircraft position, the dotted line represents the measured LOB; the continuous lines represent the sides of the LOB fan; the bold lines represent the area defined by the LOBs fans' sides; and (a), (b) and (c) represent the measured LOBs in the time domain.

Poisel [4] declared that "the idea of using maximum error is appealing because it guarantees the emitter is within the error bounds. Unfortunately, it is difficult to guarantee that there is some maximum error associated with an LOB measurement device".

In order to bypass the "maximum error guarantee" problem, we modified the MSCA technique aggregating some statistical concepts. We named our methodology as Statistical Multiple Sample Correlation Algorithm (SMSCA).

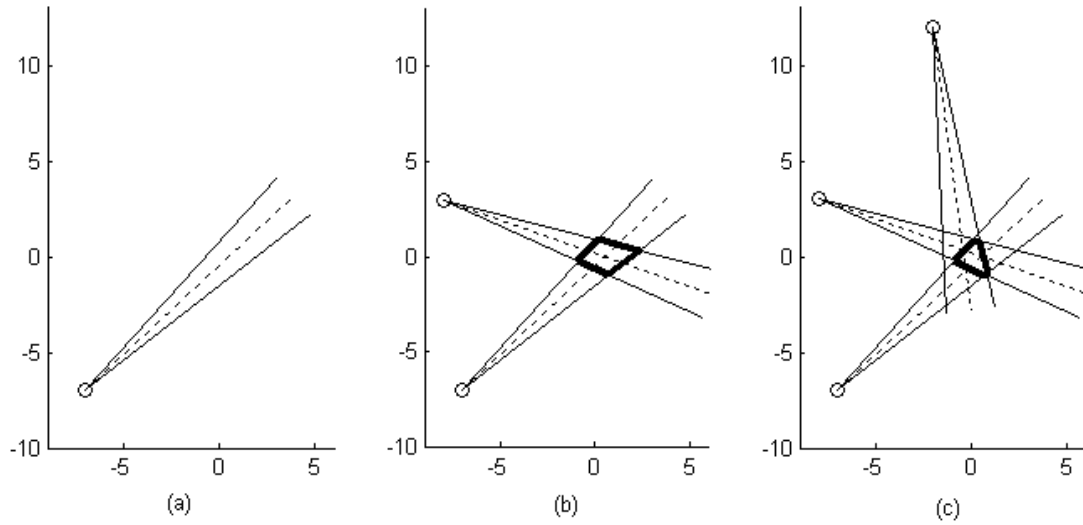


Fig. 1. MSCA basic concept

### III. STATISTICAL MULTIPLE SAMPLE CORRELATION ALGORITHM

As one can infer, the solution for the “maximum error guarantee” problem is to associate to each LOB fan a probability of the emitter to be inside it.

In order to accomplish that, we are going to assume that the total error has a Gaussian (Normal) distribution with zero mean and variance  $\sigma^2$ . We based our premise in the following statement: “in general, the central limit theorem indicates that the distribution of the sum of many random variables can be approximately normal, even though the distribution of each random variable in the sum differs from the normal” [7]. As the total error is the sum of (at least) two random variables, we believe our assumption is correct.

Given this realization, we are going to use, as LOB fan’s sides, no more the maximum error of a device, but an error related to a pre-specified probability. This idea can be visualized in figure 2, where the sides of the LOB fan

correspond to the measured LOB plus the  $p\%$  confidence limits associated to the total error probability density function, where  $p\%$  is a given probability (confidence level).

The probability of  $n$  independents events  $A_1, A_2, \dots, A_n$  occur simultaneously is:

$$P(A_1 \cap A_2 \cap \dots \cap A_n) = P(A_1)P(A_2)\dots P(A_n) \quad (1)$$

Since the  $P_{LOB}$  (emitter’s probability of lying inside one specific LOB fan) is completely independent of the probability of the emitter lying inside another LOB fan and assuming the same  $P_{LOB}$  for each LOB fan, we can rewrite (1) as:

$$P_D = P_{LOB}P_{LOB}\dots P_{LOB} = P_{LOB}^n \quad (2)$$

where  $P_D$  is the probability of the emitter lying in the area (polygon) formed by the intersection of  $n$  LOB fans with the same  $P_{LOB}$ .

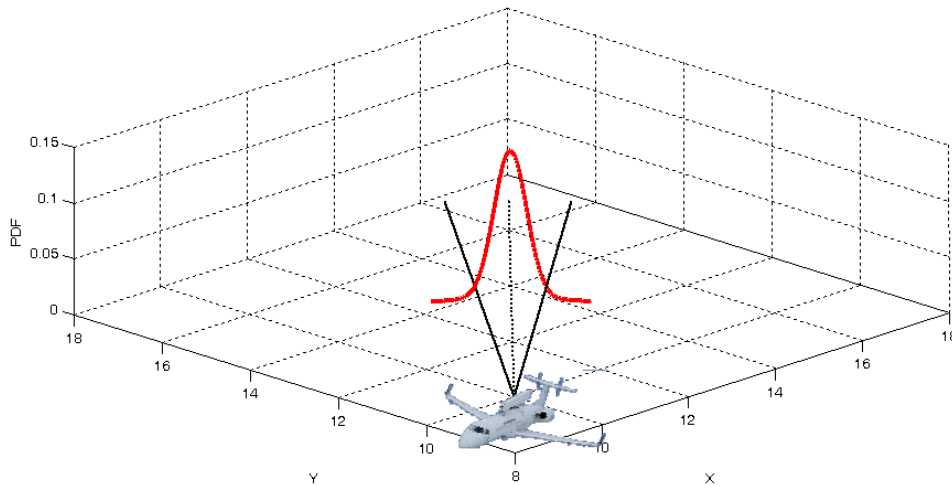


Fig. 2 Statistical sides of LOB fan

For one desired  $P_D$ , the individual probability of one LOB fan should be:

$$P_{LOB} = \sqrt[n]{P_D} \quad (3)$$

Knowing the  $P_{LOB}$  for a desired  $P_D$  and the aircraft's position, we can calculate the equations of the two sides of each LOB fan. The area that is inside all LOB fans will be the  $P_D$  error polygon. If the polygon's vertices are arranged in order to form a convex shape, the polygon's area can be calculated by (4).

$$A = \frac{1}{2} \sum_{i=0}^{n-1} (x_i y_{i+1} - x_{i+1} y_i) \quad (4)$$

The polygon's centroid coordinates are given by (5) and (6) and they will be our estimate of the emitter Position Fix (PF).

$$c_x = \frac{1}{6A} \sum_{i=0}^{n-1} (x_i + x_{i+1})(x_i y_{i+1} - x_{i+1} y_i) \quad (5)$$

$$c_y = \frac{1}{6A} \sum_{i=0}^{n-1} (y_i + y_{i+1})(x_i y_{i+1} - x_{i+1} y_i) \quad (6)$$

In (4), (5), and (6)  $n$  is the number of vertices,  $x_0 = x_n$ , and  $y_0 = y_n$ .

Our proposal can be described formally as follows:

Step 1. For a given number of LOBs and for a desired  $P_D$ , calculate the  $P_{LOB}$  through (3);

Step 2. Find the LOB fan sides by adding the measured

LOB to the  $P_{LOB}$  confidence limits associated to the total error probability density function;

Step 3. Determine the equations of the two sides of each LOB fan;

Step 4. Compute the coordinates of the  $P_D$  error polygon;

Step 5. Calculate the area and the centroid's coordinates of the  $P_D$  error polygon through (4), (5) and (6). The estimated PF will be the centroid's coordinates.

The distance between the LOB fan sides at a certain distance is proportional to the number of LOBs for a given  $P_D$ . This concept is illustrated in table I.

As the distance between the sides of the LOB fan increases with the number of LOBs, the  $P_D$  error polygon's area will increase as well. This idea can be visualized in figure 3, where in (a) we have the 95% error polygon formed by 5 LOBs and in (b) we have the same 95% error polygon formed by 3 LOBs. The notations of figure 3 are: the dotted line represents the measured LOB; the continuous lines represent the sides of LOB fan; the bold lines represent the sides of the  $P_D$  error polygon; the triangle represents the emitter's position; the circles represents the aircraft's coordinates and the asterisk represents the centroid of the polygon. Observe that the emitter's position, the aircraft's coordinates, the LOBs and the scale of the figure 3 (a) are the same ones of the figure 3 (b).

TABLE I  
INFLUENCE OF THE NUMBER OF LOBS IN THE LOB FAN ( $P_D = 0.95$  AND  $\sigma_{LOB} = 5^\circ$ ).

Number of LOBs	$P_{LOB}$ (%)	Confidence Interval	Distance between the sides of the LOB fan at 50 mi (mi)	Distance between the sides of the LOB fan at 120 mi (mi)
2	97.468	[-11.182°; 11.182°]	19.769	47.445
4	98.726	[-12.455°; 12.455°]	22.086	53.007
8	99.361	[-13.635°; 13.635°]	24.257	58.217
16	99.680	[-14.739°; 14.739°]	26.307	63.137
32	99.840	[-15.778°; 15.778°]	28.256	67.814

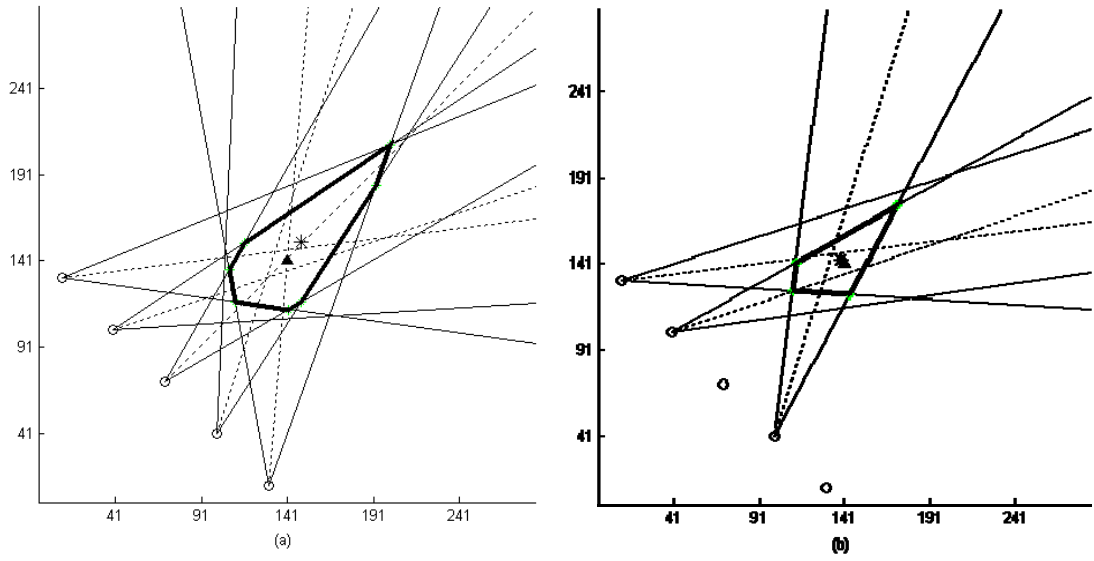


Fig. 3 Influence of the number of LOBs on the polygon's area

Based on the concept illustrated by figure 3, we offer an alternative methodology named Minimum Area Statistical Multiple Sample Correlation Algorithm (MASMSCA): perform the SMSCA for each of the  $C_{n,2} + C_{n,3} + \dots + C_{n,n}$  possible combinations of the  $n$  measured LOBs, where  $C_{n,k}$  denotes the number of combinations of  $n$  elements taken  $k$  at a time. The centroid's coordinates and the area of the polygon with the minimum area among all the combinations tested will be the outcome of the MASMSCA.

#### IV. NUMERICAL RESULTS

We simulated 2 different geometries in this section.

##### A. First Simulation

We ran 30,000 Monte Carlo simulations of the geometry proposed by [6] and [8]. This geometry was the same one illustrated in figure 3(a), where the emitter was located at (141,141) and the aircraft initial coordinates were (130,11) with a ground speed of 0.1 miles/second in each axis. The aircraft took 5 measurements (one every 300 seconds) and the

closest distance between the aircraft and the emitter was 100 miles. The total error of the measurement device was normally distributed with zero mean and standard deviation of  $1^\circ$ .

We compared the performance of our proposals (SMSCA and MASMSCA) with the Extended Kalman Filter Methodology (EKF) [8] and the original MSCA [6]. We utilized for the EKF: (135,135) as a priori estimate of the emitter position;  $diag(5^2)$  mi<sup>2</sup> as covariance matrix; and measurement uncertainty  $R = (1^\circ)^2 \text{deg}^2 = 0.0175^2 \text{rad}^2$ . For the original MSCA we used 3 degrees as maximum error of the measurement device. For our proposals we utilized a  $P_D$  of 90%. These comparisons are listed in table II.

Observe that the MASMSCA's polygon did not reach the desired  $P_D$  (90%). We noticed that, in 92% of the cases, the LOB with the maximum error was part of the LOB's combination that resulted in the polygon with the minimum area. We tribute the reason of not reaching the desired  $P_D$  to the fact that there was not anymore a Normal distribution of the error (the maximum error LOB was part of the MASMSCA polygon in most of the cases).

TABLE II  
ALGORITHMS' PERFORMANCE COMPARISON – SIMULATION 1.

Algorithm	X coordinate estimate		Y coordinate estimate		Emitter location estimate error (mi)	$P_D$ error polygon's Area (mi <sup>2</sup> )	% the emitter is inside the $P_D$ error polygon
	Mean (mi)	Standard deviation (mi)	Mean (mi)	Standard deviation (mi)			
MASMSCA	0.091	1.689	0.100	1.675	0.135	43.686	84.836
SMSCA	0.268	3.648	0.276	3.642	0.385	60.561	89.996
MSCA	0.303	1.627	0.309	1.618	0.433	102.010	98.716
EKF	-1.027	1.430	-1.306	1.635	1.661	---	---

TABLE III

Algorithm	X coordinate estimate		Y coordinate estimate		Emitter location estimate error (mi)	$P_D$ error polygon's Area (mi <sup>2</sup> )	% the emitter is inside the $P_D$ error polygon
	Mean (mi)	Standard deviation (mi)	Mean (mi)	Standard deviation (mi)			
MASMSCA	-0.001	0.786	0.015	0.787	0.015	12.806	82.042
SMSCA	0.069	2.752	0.093	2.751	0.116	25.571	93.132
MSCA	0.005	1.077	0.037	1.078	0.037	28.450	97.656
EKFM	-3.641	442.280	2.877	168.830	4.640	9.736	80.092

### B. Second Simulation

In this simulation the emitter was located at (0,0) and the aircraft took 9 LOB measures. We divided the emitter's southern hemisphere in 9 sectors of 20° each and the aircraft position at the LOB measurement time was uniformly distributed in the 80 miles arc of each sector. Acting this way, we generated 100 different geometries. Figure 4 illustrates this idea, where the continuous line represents the 80 miles arc, the dashed lines represent the borders of the nine sectors, the triangle represents the emitter, and the stars and the circles represent the aircraft's positions in 2 of the 100 generated simulations.

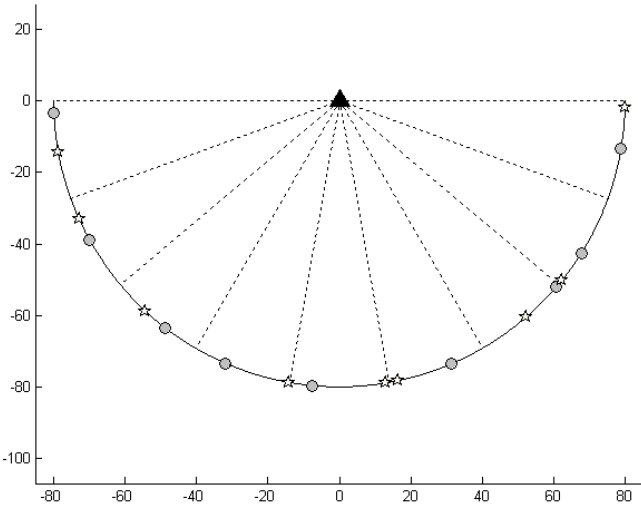


Fig. 4 Geometry of the second simulation

The parameters used in this simulation were the same ones used in the first simulation, except for:

- The geometry itself;
- We used the intersection of the first 2 LOB as a priori estimate of the emitter position for the EKFM. The other 6 LOBs were used for the EKFM itself;
- The elliptical error probable (EEP) proposed by Blachman [9] was associated to the PF estimated by the EKFM;
- A  $P_D$  of 93% was used for MASMSCA, SMSCA and Blachman's EEP.

For each of the 100 geometries we ran 5,000 Monte Carlo simulations. Table III lists the results of these 500,000 simulations.

Observe that the standard deviation of the EKFM was very big compared to the other methods. It happened because in some Monte Carlo runs the EKFM did not converged. This

lack of convergence was detected by [8] and can occur if the a priori estimate of the emitter position is too far from the real emitter's position. This situation can occur, for example, if the geometry illustrated in figure 5 takes place.

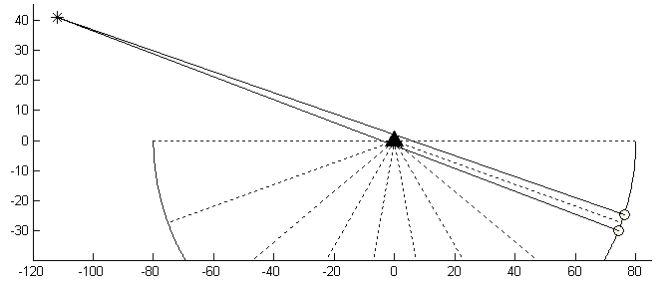


Fig. 5 Example of a far a priori estimate of the emitter position (the asterisk and the circles represent, respectively, the estimated emitter's position and the aircraft's coordinates).

The area of Blachman's EEP was smaller than the MASMSCA polygon's area but its probability of contain the emitter was also smaller than the one of MASMSCA.

Once more the MASMSCA's polygon did not reach the desired  $P_D$  (93%). The percentage of times the maximum error LOB was part of the LOB's combination that resulted in the polygon with the minimum area in this second simulation was 96%.

## V. CONCLUSION

We proposed a modification to the Multiple Sample Correlation Algorithm where some statistical concepts were aggregated to the original method. With our modifications we were able to improve the PF estimate and the  $P_D$  error polygon's area.

In section 2, we reviewed the Multiple Sample Correlation Algorithm. Our proposal was formally introduced in section 3. Section 4 presented preliminary computational results where our proposals (SMSCA and MASMSCA) were compared with the Extended Kalman Filter Methodology [8] and the original MSCA [6].

The average PF estimate calculated by MASMSCA was, at least, more than 240% closer to the real emitter position than the average PF estimate calculated by the original MSCA and, at least, more than 1,200% closer to the one computed by the EKFM.

In spite of offering a better PF estimate, the MASMSCA were not able to create an error polygon with the desired  $P_D$ .

On the other hand, the SMSCA reached the desired  $P_D$  in all the evaluated cases.

Analyzing the preliminary computational results we concluded that the best way to employ our methodology is to calculate the PF through MASMCA and the  $P_D$  error polygon boundaries by using the SMSCA.

For future works we should compare our proposal with other triangulation methods.

#### ACKNOWLEDGMENT

I would like to thank Dr. Omar José Sarmiento dos Santos for his helpful contribution.

#### REFERENCES

- [1] Doğançay, K., "On the bias of linear least squares algorithms for passive target localization", *Signal Processing*, vol. 84, issue 3, pp. 475-486, 2004.
- [2] Doğançay, K., "Bearings-only target localization using total least squares", *Signal Processing*, vol. 85, issue 9, pp. 1695-1710, Sept. 2005.
- [3] Kaplan, L. M. and Le, Q., "On exploiting propagation delays for passive target localization using bearings-only measurements", *Journal of the Franklin Institute*, vol. 342, issue 2, pp. 193-211, 2005.
- [4] Poisel, R. A., *Electronic Warfare Target Location Methods*, Norwood, MA: Artech House, 2005.
- [5] Neri, F., *Introduction to Electronic Defense Systems – Second Edition*, Norwood, MA: Artech House, 2001.
- [6] Fu, S. J., Vian, J. L., Grose, D. L., "Determination of Ground Emitter Location", *IEEE Aerospace and Electronic Systems Magazine*, vol. 3, issue 12, pp. 15-18, 1988.
- [7] DeGroot, M. H., *Probability and Statistics – Second Edition*. Addison-Wesley Publishing Company, 1987.
- [8] Spingarn, K., "Passive Position Location Estimation Using the Extended Kalman Filter", *IEEE Transactions on Aerospace and Electronic Systems*, vol. 23, issue 4, pp. 21-26, Feb. 1987.
- [9] Blachman, N. M., "On combining Target-Location Ellipses", *IEEE Transactions on Aerospace and Electronic Systems*, vol. 25, issue 2, pp. 284-287, Mar. 1989.

